Ecosystem Health and Sustainability
A SCIENCE PARTNER JOURNAL

RESEARCH ARTICLE

$\delta^{15}N$ Differences between Terricolous and Epilithic Mosses: Implications for Atmospheric Nitrogen Deposition Monitoring

Tong-Yue Deng[1,2], Yu-Ping Dong[1,2*], Yang Wang[1,2], Jia-Yi Li[2], and Lu-Lu Zhang[1,2]

[1]College of Geography and Environment, Shandong Normal University, Jinan 250358, China. [2]Institute of Environment and Ecology, Shandong Normal University, Jinan 250358, China.

*Address correspondence to: dongyuping@sdnu.edu.cn

Terricolous mosses and epilithic mosses are often used to indicate atmospheric nitrogen (N) deposition, while terricolous mosses also absorb N from soils. How to use N isotopes ($\delta^{15}N$) of terricolous mosses to trace the levels and sources of atmospheric N deposition accurately is an urgent problem to resolve. Based on the N contents (N_{moss}) and isotopes ($\delta^{15}N_{moss}$) of terricolous and epilithic mosses collected in Mount Qilian in 2022, we established a bottom-up method to calculate local atmospheric N deposition levels and source contributions. No significant difference was found in N_{moss} between soils and bare rocks, while terricolous mosses had significantly higher $\delta^{15}N_{moss}$ than epilithic mosses. Thus, the effects of soil N sources on $\delta^{15}N_{moss}$ of terricolous mosses should be excluded before they are used to trace emission sources of atmospheric N deposition. The flux of total inorganic N deposition in Mount Qilian was 15.0 ± 2.3 kg N ha^{-1} year^{-1}, with nitrate-N deposition being dominant. According to analyses of emission sources, it was volatilization-related ammonia (61.9%$\pm$19.8%; mainly from fertilizer application and wastes) rather than combustion-related ammonia (38.1%$\pm$19.8%) that dominated atmospheric ammonium-N deposition. It was fossil fuel N oxides (51.5%$\pm$19.6%; mainly from oil and coal combustion) rather than non-fossil fuel N oxides (48.5%$\pm$19.6%; mainly from biomass burning and microbial N cycles) that dominated nitrate-N deposition in this region. The Mount Qilian region holds an important position as a crucial ecological barrier in western China. Therefore, it is important to reduce reactive N emissions based on the above source apportionments to protect the fragile ecosystems of Mount Qilian.

Citation: Deng T-Y, Dong Y-P, Wang Y, Li J-Y, Zhang L-L. $\delta^{15}N$ Differences between Terricolous and Epilithic Mosses: Implications for Atmospheric Nitrogen Deposition Monitoring. *Ecosyst. Health Sustain.* 2025;11:Article 0458. https://doi.org/10.34133/ehs.0458

Submitted 5 August 2025
Revised 5 November 2025
Accepted 26 November 2025
Published 16 December 2025

Introduction

Atmospheric nitrogen (N) deposition, as a global hotspot issue, has always attracted much attention. In recent years, thanks to a series of policies implemented by the government, anthropogenic atmospheric N deposition has gradually declined [1,2]. From 2012 to 2020, annual total N deposition (sum of dry and wet deposition) was estimated to continuously decline in China by about 23%, while the flux of total N deposition was still high at 39.2 ± 2.42 kg N ha^{-1} year^{-1} during 2011 to 2020 [3]. There was still high anthropogenic reactive N emitted into ecosystems, leading to adverse effects including the decrease of biodiversity and soil acidification [4]. Therefore, it is important to monitor the levels and trace the sources of atmospheric N deposition.

The National Atmospheric Nitrogen Deposition Monitoring Network (NNDMN), established by China Agricultural University, covered 66 monitoring sites [1]. However, the number of monitoring sites in northwestern China is limited, posing challenges for the accurate quantification of atmospheric N deposition in this region [5]. Mount Qilian (Mt. Qilian) is located on the edge of the Qinghai–Tibet Plateau and serves a critical role against the encroachment of surrounding deserts [6]. Based on the calculation of an atmospheric chemical transport model, the flux of atmospheric N deposition in Mt. Qilian was approximately 10 to 20 kg N ha^{-1} year^{-1} in 2018 [7]. At a 3,200-m altitude in Mt. Qilian, the concentrations of soil ammonium-N and soil nitrate-N in August were 11.79 ± 3.57 and 5.68 ± 0.87 mg kg^{-1}, respectively [8]. The western part of Mt. Qilian features large areas of bare land, sandy land, and gobi with low surface vegetation coverage and harsh natural conditions, belonging to the alpine semiarid ecosystem [6]. In an alpine ecosystem on the eastern margin of the Qinghai–Tibet Plateau, the N critical load (considering plant cover and biomass change) ranges between 8.8 and 12.7 kg N ha^{-1} year^{-1} [9]. Therefore, the levels and sources of atmospheric N pollution are crucial information for protecting the fragile ecosystems of the Mt. Qilian region.

Mosses, lacking developed root systems and protective cuticle, could adsorb N directly from atmosphere [10,11] and are widely regarded as bioindicators for atmospheric N deposition [4]. Thus, moss N contents (N_{moss}) are widely used to quantify atmospheric N deposition [12–14]. In China, the N_{moss} in eastern coastal areas (e.g., Jiangsu and

Zhejiang) is generally higher than that in western inland areas (e.g., Sichuan and Yunnan) [13,14], which is highly consistent with the spatial distribution of regional atmospheric N deposition [5]. In Europe, the N_{moss} is positively correlated with the atmospheric N deposition simulated by the EMEP (European Monitoring and Evaluation Programme) model [15]. During 2005 to 2010, the N_{moss} decreased in countries such as Belgium, Slovenia, and Macedonia, while it continued to rise in Germany, Spain, and the United Kingdom [10,16]. These differences in N_{moss} among countries may be closely associated with the implementation of targeted pollution control measures and regional N emission policies.

The N isotopes of mosses ($\delta^{15}N_{moss}$) serve as a traceability tool for atmospheric N pollution, since major N emission sources have significantly different $\delta^{15}N$ signatures [17,18]. For example, in the rural areas of Europe, increased NH_3 emissions from agriculture and livestock activities resulted in a decrease in moss $\delta^{15}N$ values in the late 20th century [19]. In Southwest China, the $\delta^{15}N_{moss}$ were used to quantitatively differentiate source contributions to atmospheric N deposition [13]. Furthermore, the N acquisition mechanism of mosses shows significant interspecific differences and environmental adaptability [20,21]. At the same sampling area with identical atmospheric N deposition conditions, the $\delta^{15}N_{moss}$ values of terricolous mosses (growing on soils) under canopies were significantly lower than those in open fields [22]. Epilithic mosses (growing on bare rocks) nearly exclusively obtain N through atmospheric N deposition and are less affected by rock substrates [22,23]. With no developed root system and protective cuticle, mosses can directly absorb inorganic N from the thin surface layer of soils into their tissues via surface cells [24]. The NH_4^+ and NO_3^- can easily enter moss tissues through the proton (H^+) pump and cation exchange, and cotransport with positively charged ions, respectively [24]. In Guiyang, terricolous mosses had higher $\delta^{15}N_{moss}$ values than those of epilithic mosses, and about 37% in terricolous moss N was derived from soils [25]. Therefore, the effects of soil N sources on the $\delta^{15}N_{moss}$ of terricolous mosses should be considered when they are used to quantify contributions of emission sources to atmospheric N deposition.

Currently, studies on atmospheric N deposition are primarily focused on regions with intensive anthropogenic activities, and fewer studies have been conducted in northwestern China. Mt. Qilian is a critical ecological barrier in northwestern China. The major objectives of our study are to (a) analyze the effects of different growth substrates (soils and bare rocks) on moss N enrichment and (b) estimate the levels and sources of atmospheric N deposition in Mt. Qilian.

Materials and Methods

Study area

Mt. Qilian is located in northwestern China, at the border between Gansu and Qinghai provinces, with geographical coordinates of 36°30′N to 39°30′N, 93°30′E to 103°E. The total area is approximately 18.1 × 10^4 km^2. The mean annual precipitation in this region is 300 to 700 mm, with a typical feature of continental climate [6]. The vegetation types in this area exhibit distinct vertical zonation [6,26]. Our study area is situated in the west of Mt. Qilian, within Gansu Province (Fig. 1). The altitude of the sample plots ranges from 3,160 to 3,960 m (Fig. 1). It is reported that there are a total of 327 species of mosses belonging to 126 genera and 38 families in the Mt. Qilian area [27]. The dominant moss families mainly include *Pottiaceae*, *Bryaceae*, *Hypnaceae*, and *Brachytheciaceae*, among others. [28]. The spatial distribution pattern of mosses in Mt. Qilian is patchy, with a large distribution range and spatial heterogeneity, and a low patch connectivity [29].

Sample collection

Moss samples were collected from Mt. Qilian in July and August 2022. The sampling sites were all located in natural open habitats without tree cover, insect interference, serious pollution, or frequent anthropogenic disturbances. During sampling, it was important to preserve the integrity of moss samples while avoiding excessive collection. The detailed information of collection sites, including longitude and latitude, and substrate types, was recorded promptly (Table S1). Four to six subsamples were mixed to generate one typical sample per sampling site for subsequent analyses. The new tissues of moss samples on soils (terricolous mosses; n = 11) and bare rocks (epilithic mosses; n = 5) were collected in Mt. Qilian for experimental analyses.

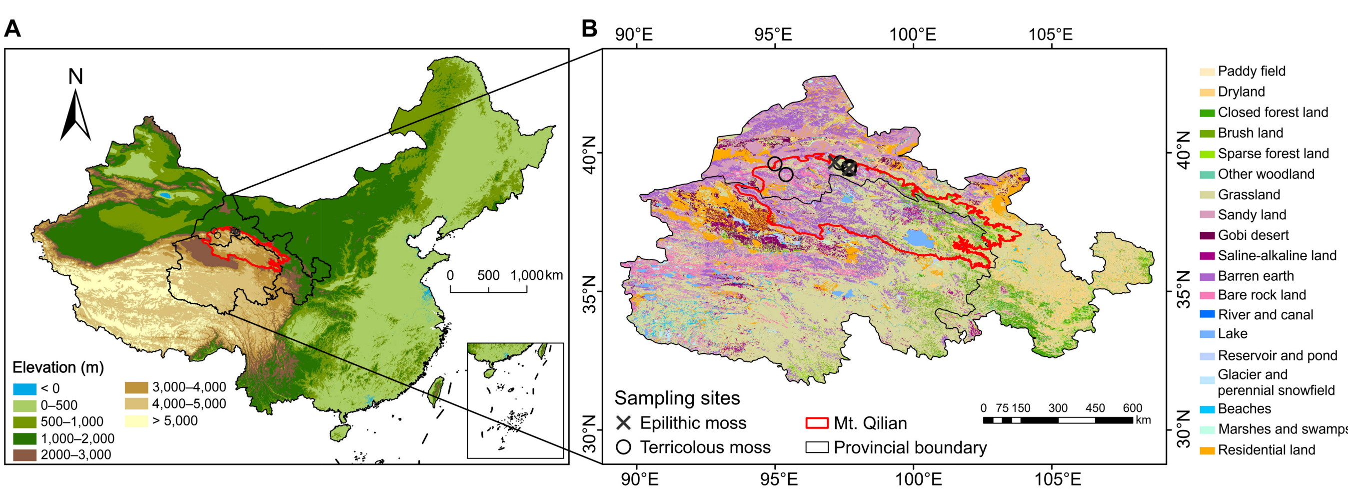

Fig. 1. Study area. (A) Location of sampling sites in China. (B) Sampling sites of terricolous and epilithic mosses of Mt. Qilian in northwestern China. The underlying surface information includes elevation distribution and China's 2020 second-level land use types (Resource and Environmental Science Data Platform, Chinese Academy of Sciences: https://www.resdc.cn/).

Experimental analysis

Using deionized water, we washed moss samples several times until no N was detected in the rinsing water. The cleaned samples were dried in a vacuum oven at 70 °C and subsequently ground into powder [30]. The N_{moss} (%, dry weight) were determined by an elemental analyzer (PE2400 II, USA) with an analytical precision of 0.1%. The $\delta^{15}N_{moss}$ values were measured on a combined isotope ratio mass spectrometer (Thermo Scientific MAT 253) and elemental analyzer (Flash EA 2000). IAEA-N-1 (ammonium sulfate, $\delta^{15}N = 0.4‰$), IAEA-NO-3 (potassium nitrate, $\delta^{15}N = 4.7‰$), and USGS25 (ammonium sulfate, $\delta^{15}N = -30.4‰$) standard samples were used to calibrate the $\delta^{15}N_{moss}$ values of samples. The natural abundance of ^{15}N was calculated as $\delta^{15}N$ values in parts per mil (‰):

$$\delta^{15}N = \left(R_{sample}/R_{standard} - 1\right) \times 1{,}000 \quad (1)$$

where R represents $^{15}N/^{14}N$ in moss samples and standard samples (atmosphere N_2).

Fractions of soil and atmospheric N sources to terricolous moss N

Epilithic mosses are common bio-monitors, absorbing N almost exclusively from atmosphere [22,23]. Due to terricolous mosses absorbing N from soils, their $\delta^{15}N_{moss}$ values tend to be higher than those of epilithic mosses on bare rocks in the same study area [31]. We assumed that the entry of N into moss tissues has no substantial ^{15}N fractionation [32]. Therefore, to eliminate the influence of soil N sources on the $\delta^{15}N_{moss}$ values of terricolous mosses, we updated a method to calculate the proportion of both soil and atmospheric N sources in the N_{moss} of terricolous moss tissues (Fig. S1).

We assumed that all the N_{moss} of epilithic mosses is derived from atmospheric N deposition and all the N_{moss} of terricolous mosses is derived from atmospheric N deposition and soils. Atmospheric N deposition is composed of dry deposition (the sum of NH_3 and NO_2, denoted as d-NH_3 and d-NO_2, respectively) and wet deposition (the sum of NH_4^+ and NO_3^-, denoted as w-NH_4^+ and w-NO_3^-, respectively), which serve as potential atmospheric N sources for mosses. In addition, soil NH_4^+ and NO_3^- (s-NH_4^+ and s-NO_3^-, respectively) serve as additional N sources for terricolous mosses. The flux-weighted $\delta^{15}N$ of atmospheric N deposition ($\delta^{15}N_{atm\text{-}N}$) and soil N ($\delta^{15}N_{soil\text{-}N}$) was calculated by using Eqs. 2 and 3.

$$\delta^{15}N_{atm-N} = \delta^{15}N_{d-NH3} \times f_{d-NH3} + \delta^{15}N_{d-NO2} \times f_{d-NO2} + \delta^{15}N_{w-NH4+} \times f_{w-NH4+} + \delta^{15}N_{w-NO3-} \times f_{w-NO3-} \quad (2)$$

where the $f_{d\text{-}NH3}$, $f_{d\text{-}NO2}$, $f_{w\text{-}NH4+}$, and $f_{w\text{-}NO3-}$ were fractions of d-NH_3, d-NO_2, w-NH_4^+, and w-NO_3^- in atmospheric N deposition, and we assumed that $f_{d\text{-}NH3} + f_{d\text{-}NO2} + f_{w\text{-}NH4+} + f_{w\text{-}NO3-} = 1$ (detailed in Table 1). The $\delta^{15}N_{d\text{-}NH3}$, $\delta^{15}N_{d\text{-}NO2}$, $\delta^{15}N_{w\text{-}NH4+}$, and $\delta^{15}N_{w\text{-}NO3-}$ values are detailed in Table 1. The $\delta^{15}N_{atm\text{-}N}$ value is shown in Table 1.

$$\delta^{15}N_{soil-N} = \delta^{15}N_{s-NH4+} \times f_{s-NH4+} + \delta^{15}N_{s-NO3-} \times f_{s-NO3-} \quad (3)$$

where the $f_{s\text{-}NH4+}$ and $f_{s\text{-}NO3-}$ were fractions of s-NH_4^+ and s-NO_3^- in soil N and we assumed that $f_{s\text{-}NH4+} + f_{s\text{-}NO3-} = 1$ (detailed in Table 1). The $\delta^{15}N_{s\text{-}NH4+}$ and $\delta^{15}N_{s\text{-}NO3-}$ values are detailed in Table 1. The $\delta^{15}N_{soil\text{-}N}$ value is shown in Table 1.

Table 1. The $\delta^{15}N$ values and fractions of dominant N sources for mosses

N species	$\delta^{15}N$ values (‰)	Fractions (%)
d-NH_3	-13.4 ± 6.2[a]	29.4[b]
d-NO_x	-8.2 ± 3.9[a]	5.5[b]
w-NH_4^+	-2.6 ± 3.9[a]	39.2[b]
w-NO_3^-	-0.3 ± 4.1[a]	25.9[b]
s-NH_4^+	6.2 ± 1.1[c]	85.3[c]
s-NO_3^-	-0.6 ± 0.8[c]	14.7[c]
atm-N	-5.5 ± 4.6	74.3 ± 7.5
soil-N	5.2 ± 1.0	25.7 ± 7.5

[a]The $\delta^{15}N$ values of atmospheric N species were obtained from Ref. [47].

[b]Fractions of N species in atmospheric N deposition were calculated based on observed fluxes of atmospheric N deposition [48].

[c]The $\delta^{15}N$ values and fractions of soil N species in soil N were calculated based on observed $\delta^{15}N$ values and concentrations of NH_4^+ and NO_3^- in mossy soils [25].

Then, the 2-end-member mixing model was used for terricolous mosses. The fractions of atm-N and soil-N ($f_{atm\text{-}N}$ and $f_{soil\text{-}N}$) in terricolous mosses were calculated by using Eq. 4.

$$\delta^{15}N_{moss} = \delta^{15}N_{atm-N} \times f_{atm-N} + \delta^{15}N_{soil-N} \times f_{soil-N} \quad (4)$$

where we assumed that $f_{atm\text{-}N} + f_{soil\text{-}N} = 1$.

The $\delta^{15}N_{moss}$ of epilithic mosses and terricolous mosses from [25] were used to prove the usability of our method (Table S3). We also collected epilithic mosses in Mt. Qilian for comparison. No significant difference in $\delta^{15}N$ values was observed between terricolous (after removing soil-N) and epilithic mosses in both Mt. Qilian and Guiyang (Table S3).

Fractions and fluxes of major N emission sources to total N deposition

Based on the fluxes of total atmospheric N deposition (F_{TN}) in northwest China (Table S2) and the N_{moss} of *Grimmia* mosses in Mt. Qilian, we updated an empirical formula between N_{moss} and atmospheric N deposition in Mt. Qilian (shown in Text S1). The ratios of NH_x to NO_y in total N deposition (NH_x/NO_y, denoted as K) were calculated using the empirical relationship between the K and $\delta^{15}N_{moss}$ values [12]. The fluxes of NH_x (F_{NHx}) and NO_y (F_{NOy}) deposition were estimated using the above F_{TN} and K values. Based on K values, we calculated the fractions of NH_x (f_{NHx}) and NO_y (f_{NOy}) deposition relative to total N deposition. Then, we calculated the $\delta^{15}N$ values of NH_x and NO_y deposition ($\delta^{15}N_{NHx}$ and $\delta^{15}N_{NOy}$) using a convex optimization model (CVXPY) and the corresponding initial $\delta^{15}N$ values of NH_3 and NO_x emissions ($\delta^{15}N_{i\text{-}NH3}$ and $\delta^{15}N_{i\text{-}NOx}$). Finally, the fractions of volatilization ($f_{v\text{-}NH3}$) and combustion ($f_{c\text{-}NH3}$) sources in total NH_3 emissions and the fractions of fossil fuel ($f_{f\text{-}NOx}$) and non-fossil fuel ($f_{nf\text{-}NOx}$) sources in total

NO_x emissions (Table S5) were calculated. Additionally, the fluxes of c-NH_3 ($F_{c\text{-}NH3}$) and v-NH_3 ($F_{v\text{-}NH3}$) to NH_x deposition and the fluxes of f-NO_x ($F_{f\text{-}NOx}$) and nf-NO_x ($F_{nf\text{-}NOx}$) to NO_y deposition were quantified [18].

Statistical analysis

GetData was used for data acquisition. Data analysis was conducted with GraphPad Prism 9.5.0 and Origin 2024. The Shapiro–Wilk test was used to verify the normality of the data and found that the data followed a normal distribution ($P > 0.05$). The Levene test was employed to verify the homogeneity of variances and found that the variances of each group of data were homogeneous ($P > 0.05$). Independent samples t tests were employed to evaluate the differences in N_{moss}, $\delta^{15}N_{moss}$, and estimated $f_{v\text{-}NH3}$, $f_{c\text{-}NH3}$, $f_{f\text{-}NOx}$, and $f_{nf\text{-}NOx}$ between terricolous and epilithic mosses. Additionally, t tests were used to compare $\delta^{15}N_{moss}$ differences between terricolous mosses (after removing the part of soil N) and epilithic mosses. The significance level was set at $p < 0.05$.

Results

Nitrogen contents and isotopes of mosses on different substrates

In Mt. Qilian, the N contents of terricolous mosses (1.6 ± 0.3%; range: 1.3% to 2.0%) were comparable with those of epilithic mosses (1.6 ± 0.1%, range: 1.4% to 1.7%) (Fig. 2A). The $\delta^{15}N_{moss}$ values of terricolous mosses (−2.7‰ ± 0.8‰) were significantly higher than those of epilithic mosses (−4.0‰ ± 0.8‰) (Fig. 2B).

Fluxes of atmospheric N deposition at Mt. Qilian

Combining the F_{TN} (15.0 ± 2.3 kg N ha^{-1} $year^{-1}$) for Mt. Qilian (Fig. 3A and Table S2), the F_{NHx} and F_{NO_y} for the same year were determined to be 6.9 ± 1.0 and 8.1 ± 1.2 kg N ha^{-1} $year^{-1}$, respectively. The NO_y-N accounted for 54.0% of the total inorganic N deposition, indicating that NO_y-N dominated the atmospheric N deposition in this region (Fig. 3B).

Sources of atmospheric N deposition at Mt. Qilian

The $f_{v\text{-}NH3}$ in atmospheric NH_x deposition was 61.9% ± 19.8%, which was significantly higher than $f_{c\text{-}NH3}$ (accounting for 38.1% ± 19.8%) in Mt. Qilian. In addition, $f_{f\text{-}NOx}$ in atmospheric NO_y deposition was 51.5% ± 19.6%, which was slightly higher than $f_{nf\text{-}NOx}$ (accounting for 48.5% ± 19.6%) in Mt. Qilian (Fig. 4A). The $F_{v\text{-}NH3}$ (4.3 ± 0.6 kg N ha^{-1} $year^{-1}$) was slightly higher than $F_{f\text{-}NOx}$ (4.2 ± 0.6 kg N ha^{-1} $year^{-1}$), $F_{nf\text{-}NOx}$ (3.9 ± 0.6 kg N ha^{-1} $year^{-1}$), and $F_{c\text{-}NH3}$ (2.6 ± 0.4 kg N ha^{-1} $year^{-1}$) (Fig. 4B).

Discussion

Comparison of the N_{moss} and $\delta^{15}N_{moss}$ on different substrates

In Mt. Qilian, no significant difference in the N_{moss} was found between mosses on soils (1.6% ± 0.3%) and bare rocks (1.6% ± 0.1%) in the present study (Fig. 2A). This indicates that epilithic and terricolous mosses had similar N availability.

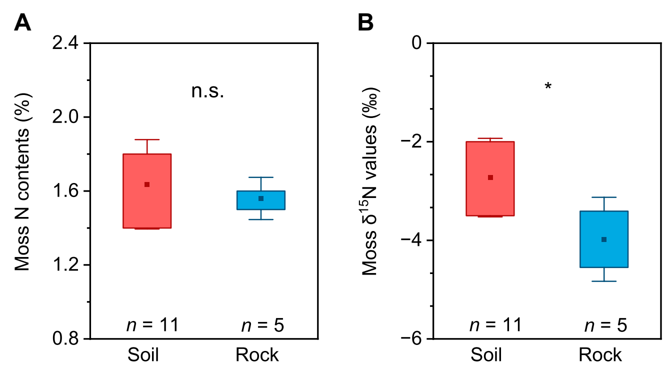

Fig. 2. Moss (A) N contents and (B) $\delta^{15}N$ values on soils ($n = 11$) and bare rocks ($n = 5$) in Mt. Qilian. The red and blue squares within the box represent the mean values, each box encompasses the 25th to 75th percentiles of data range, and the whiskers represent the range of SD. n.s. represents no significant difference ($P > 0.05$). * represents significant difference ($P < 0.05$).

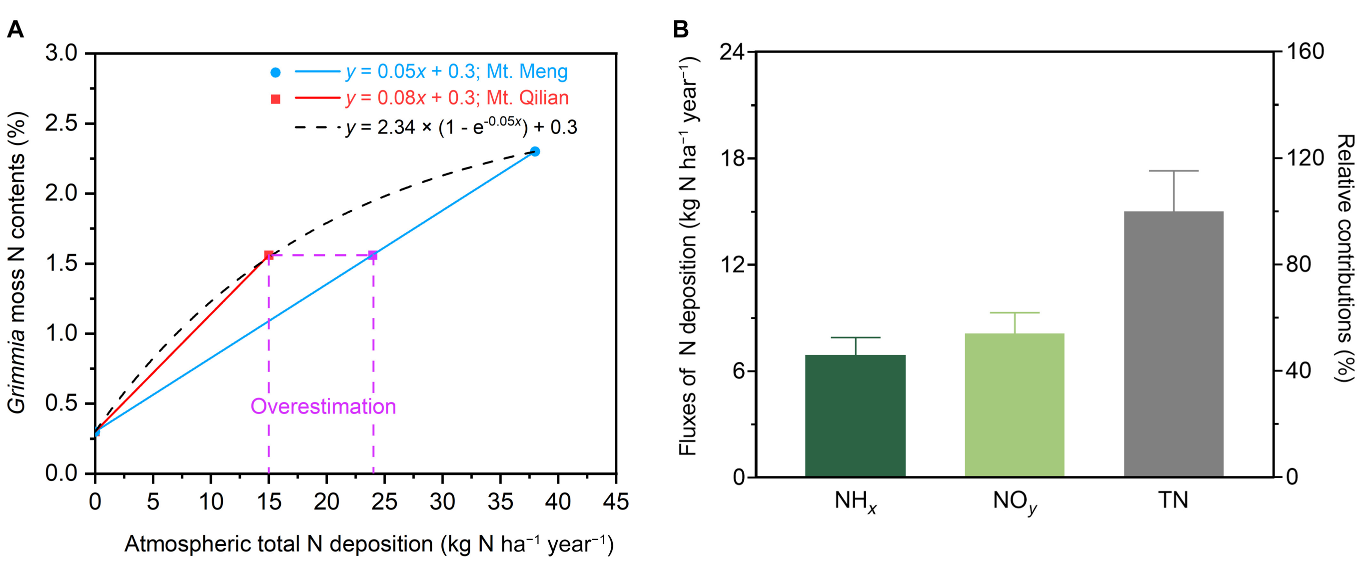

Fig. 3. *Grimmia* moss N contents and atmospheric N deposition in Mt. Qilian. (A) The empirical relationships between *Grimmia* moss N contents and the fluxes of total atmospheric N deposition at Mt. Meng in 2018 [18] and Mt. Qilian in 2022. (B) The fluxes and contributions of NH_x, NO_y, and total N deposition (TN) at Mt. Qilian.

Furthermore, the N_{moss} on sandstones and limestones showed no significant difference in the Huanjiang Karst area of Guangxi [21]. This might be related to N utilization mechanism and capabilities of nutrient uptake and transport.

The $\delta^{15}N_{soil\text{-}N}$ values were higher than $\delta^{15}N_{atm\text{-}N}$ (Table 1). In this study, the $\delta^{15}N_{moss}$ values of terricolous mosses (−2.7‰ ± 0.8‰) were significantly higher than those of epilithic mosses (−4.0‰ ± 0.8‰) (Fig. 2B). This is consistent with the fact that the $\delta^{15}N$ values of terricolous mosses were higher than those of epilithic mosses in several observations (Table 2). These results support that terricolous mosses obtain N from soils (with more positive $\delta^{15}N$ values). In addition to the influence of soil N sources on $\delta^{15}N_{moss}$ signatures, it may also be related to the morphological characteristics of mosses, the preference for nutrient absorption of mosses, and the levels of regional NH_3 and NO_x emissions [33]. Thus, the influences of soil N sources in $\delta^{15}N_{moss}$ of terricolous mosses should be excluded before they are used to trace emission sources of atmospheric N deposition. In the future, more experimental studies are required to eliminate uncertainties to improve the accuracy when using terricolous mosses to indicate atmospheric N deposition.

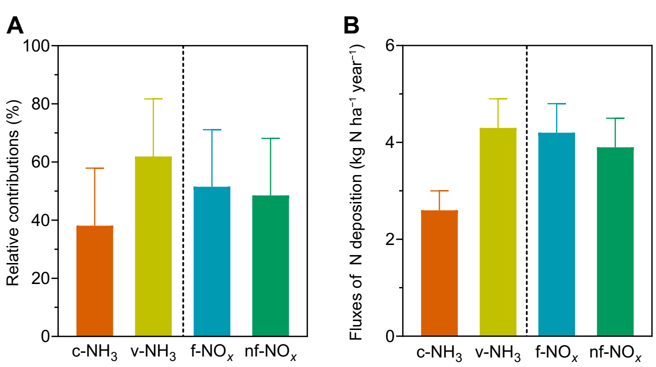

Fig. 4. Relative and real contributions of major emission sources to atmospheric N deposition. (A) Relative contributions of c-NH_3 and v-NH_3 emissions to atmospheric NH_x deposition, and relative contributions of f-NO_x and nf-NO_x emissions to atmospheric NO_y deposition. (B) The fluxes of c-NH_3, v-NH_3, f-NO_x, and nf-NO_x emissions to atmospheric N deposition at Mt. Qilian in 2022. Mean ± SD is shown.

The relationship between atmospheric N deposition and the N_{moss}

Generally, the N_{moss} increases with the levels of atmospheric N deposition [4,12,15,34]. In Mt. Qilian, the N_{moss} of *Grimmia* mosses was 1.5% ± 0.2% (Fig. 3A) and F_{TN} was 15.0 ± 2.3 kg N ha^{-1} year^{-1} (Table S2). The N_{moss} in most nonurban regions of China were higher than those in Mt. Qilian (1.6% ± 0.3%) and Mt. Gongga (1.1% ± 0.3%) (Table 2). In suburban regions of Jiangxi Province, the N_{moss} reached 2.6% ± 0.2% in 2010 (Table 2). Geographically, the N_{moss} generally showed a distribution pattern of being higher in east and lower in west in China (Table 2), which was consistent with the spatial heterogeneity of atmospheric N deposition across the country. The atmospheric reactive N deposition in China gradually decreases from the densely populated eastern regions to the western region [3,35]. Between 2000 and 2010, the differences in gross regional product and industrial structure led to an imbalance in NO_x emissions between eastern and western regions [36]. The N_{moss} from Mt. Meng (2.4% ± 0.3%) and Mt. Tai (2.1% ± 0.4%) areas in Shandong were higher than those in Mt. Qilian (1.6% ± 0.1%) of northwestern China (Table 2). The intensive agricultural activities, N fertilizer application, and the increase of vehicle population and coal consumption have significantly increased emissions of regional atmospheric N pollution in Shandong [14,37]. The pollution-intensive industries and energy consumption in Shandong have contributed to its high levels of atmospheric N pollution. In contrast, the low N_{moss} at Mt. Qilian indicated the level of atmospheric N pollution in this area was relatively low.

Linear relationships between the N_{moss} and atmospheric N deposition fluxes have been established in many studies [15,38,39]. However, the response of the N_{moss} to atmospheric N deposition under low levels may be more sensitive than under high N deposition [10,15]. Thus, the relationships between the N_{moss} and atmospheric N deposition fluxes should be asymptotic [10,15]. Consequently, the linear relationship established in the Mt. Meng region with high N deposition will overestimate the F_{TN} in Mt. Qilian (Fig. 3A). In 2022, the observed F_{TN} (15.0 ± 2.3 kg N ha^{-1} year^{-1}; Table S2) in Mt. Qilian is close to the critical N load of the northwest desert steppe ecosystem (15 to 30 kg N ha^{-1} year^{-1}) [40], and lower than F_{TN}

Table 2. Moss N contents (N_{moss}) and $\delta^{15}N$ values ($\delta^{15}N_{moss}$) in nonurban regions of China. *n* represents sample size. – represents not available.

Year	Region	*n*	Substrates	N_{moss} (%)	$\delta^{15}N_{moss}$ (‰)	References
2006	Rural, Guiyang	–	Rock	1.3 ± 0.1	−3.6 ± 1.0	[12]
2010	Suburban, Jiangxi	46	Rock	2.6 ± 0.2	−3.3 ± 0.8	[49]
2021	Mt. Tai	16	Rock	2.1 ± 0.4	−5.2 ± 2.4	[14]
2022	Mt. Meng	9	Rock	2.4 ± 0.3	−9.6 ± 1.3	[18]
2022	Mt. Qilian	5	Rock	1.6 ± 0.1	−4.0 ± 0.8	This study
2022	Mt. Qilian	11	Soil	1.6 ± 0.3	−2.7 ± 0.8	This study
2008	Huanjiang	9	Soil	1.4 ± 0.3	−2.3 ± 1.0	[21]
2008	Huanjiang	12	Soil	1.4 ± 0.2	0.1 ± 0.7	[21]
2007	Mt. Gongga	14	Soil	1.1 ± 0.3	−1.4 ± 2.2	[38]

(39.9 kg N ha^{-1} $year^{-1}$) in Mt. Meng [18]. The F_{NO_y}, which accounted for 54.0% of the total inorganic N deposition, was higher than F_{NH_x} in Mt. Qilian (Fig. 3B). This is contrary to the situation in rural areas of northwest China where NH_x-N dominates [30]. This might be due to the environmental improvement of Mt. Qilian in recent years, such as the closure of several mining sites and hydroelectric power stations [41]. However, the Mt. Qilian area suffers from severe soil erosion, sparse vegetation, and a fragile ecological environment [6]. Once damaged, it will be extremely difficult to recover. Therefore, in order to protect the fragile ecosystems in this region, it is urgent to make measures to control NH_3 and NO_x emissions.

Emission sources of atmospheric N deposition in Mt. Qilian

The $\delta^{15}N$ values are important tools for studying N cycle and tracing N sources, and their differences usually reflect the processes of N sources, transformations, and distributions in ecosystems [21]. For example, aquatic plants (reed and calamus) exhibited significant differences in absorbing different N forms, and their $\delta^{15}N$ characteristics can be used to trace N sources [42]. For atmospheric NH_x deposition, $f_{v\text{-}NH3}$ (61.9% ± 19.8%) was significantly higher than $f_{c\text{-}NH3}$ (38.1% ± 19.8%) in Mt. Qilian (Fig. 4A). This indicates that agricultural activities (e.g., livestock farming) may be the dominant source of NH_3 emissions in Mt. Qilian. Combined with the characteristics of the economic structure of the western region, the development of Mt. Qilian area is highly dependent on animal husbandry, mineral resources development, and ecotourism [43]. The NH_3 volatilization (accounting for 63% in 2017) caused by increased N fertilizer application and direct emission of animal manure is the main pathway of N emission into the environment [44]. According to the Gansu Provincial Statistical Yearbook (https://tjj.gansu.gov.cn/), it was seen that livestock farming in Gansu Province increased during 2008 to 2022, with sheep having the highest growth rate of 46.6%. Compared to 2021, the sown area of crops increased by 1.6% in 2022. Notably, organic fertilizers (e.g., livestock manure) are widely used in agricultural production in Mt. Qilian area. Although this traditional fertilization method has environmental advantages, it may also lead to an increase in NH_3 emissions, which could potentially impact the quality of regional atmospheric environment. For atmospheric NO_y deposition, $f_{f\text{-}NO_x}$ was slightly higher than $f_{nf\text{-}NO_x}$ in Mt. Qilian (Fig. 4A). This indicates that fossil fuel NO_x sources (e.g., industry and transportation) contribute slightly more to total NO_x emissions than non-fossil fuel NO_x sources. With the increase in resource development, mining and energy development form the core of the region's industrial economy, leading to an increase in NO_x emissions from f-NO_x sources. The development of eco-tourism has injected new vitality into the regional economy [43]. However, while these activities promote regional economic development, they also have a greater impact on natural resources and ecological environment. The $F_{v\text{-}NH3}$ is higher than those of the other 3 sources ($F_{f\text{-}NO_x}$, $F_{nf\text{-}NO_x}$, and $F_{c\text{-}NH3}$), followed by $F_{f\text{-}NO_x}$ (Fig. 4B). Therefore, we should pay more attention to control v-NH_3 and f-NO_x emissions in this area. In addition, the standard deviations of the $\delta^{15}N$ values for each NH_3 and NO_x emission sources, sampling mosses, soil N sources of mosses, and the isotope effects during transportation and transformation processes in atmosphere would be reflected in source apportionment results. The high standard deviations in source apportionment results reflect considerable uncertainty.

Although the $\delta^{15}N_{moss}$ is widely used to trace the levels, compositions, and sources of atmospheric N deposition, it still has some uncertainties. In this study, we assumed that all N_{moss} of epilithic mosses is derived from atmospheric N deposition. Our sample size was relatively small, and the distribution of mosses in Mt. Qilian is uneven and high heterogeneity. Therefore, it is worthwhile to increase the sample size in future work to mitigate these uncertainties. Meanwhile, more field observations in different habitats are warranted to explore the N acquisition and utilization mechanisms of terricolous and epilithic mosses. The 2-end-member mixing model is used for terricolous mosses, and there are still many uncertain factors in calculations, such as microbial activities, moss N utilization mechanisms, and the isotope fractionation effects during multiple N transformation and transportation processes in atmosphere and soils [21,45]. In addition to atmospheric and soil N sources, some mosses could fix N_2 by forming symbiotic relationships with N_2-fixing bacteria (such as cyanobacteria). Nevertheless, the N addition of 4.3 kg N ha^{-1} $year^{-1}$ could inhibit N_2 fixation in mosses [46]. The atmospheric N deposition in our study area was 15.0 ± 2.3 kg N ha^{-1} $year^{-1}$; thus, the contributions of N_2 fixation to moss N were not considered in this study. Moreover, the $\delta^{15}N$ values of emission sources derived from literatures may not fully reflect site-specific conditions. In future research, more attention should be paid to accurately quantifying atm-N and soil-N sources in different habitats of the study area. This will help optimize the mixed model and improve the accuracy of tracing method.

Conclusion

We updated an isotope method for tracing emission sources of atmospheric N deposition using terricolous mosses. This work fills the gap in monitoring the levels and sources of atmospheric N deposition by mosses in northwest China. In 2022, the flux of total inorganic N deposition in Mount Qilian was 15.0 ± 2.3 kg N ha^{-1} $year^{-1}$. The F_{NO_y} is significantly higher than F_{NH_x}, indicating that NO_y deposition is dominant in total N deposition. The fraction of v-NH_3 is higher than that of c-NH_3 in NH_x deposition. In NO_y deposition, the fraction of f-NO_x is slightly higher than that of nf-NO_x, which is related to the local characteristic agriculture, animal husbandry, and mining activities. In the future, this method can be further optimized and extended to more regions, which will provide scientific support for formulating targeted ecological protection and pollution control strategies.

Acknowledgments

We would like to gratefully thank Prof. Xue-Yan Liu of Tianjin University for his thought-provoking discussion. We also gratefully thank Dr. Ling Hu of Shandong Normal University for her assistance on field works.

Funding: This research was supported by the National Natural Science Foundation of China (42003011).

Author contributions: T.-Y.D.: Methodology, data curation, formal analysis, and writing—original draft. Y.-P.D.: Funding acquisition, methodology, data curation, formal analysis, conceptualization, supervision, and writing—review and editing. Y.W.: Methodology, data curation, and writing—review and editing. J.-Y.L.: Investigation and writing—review and editing. L.-L.Z.: Supervision and writing—review and editing.

Competing interests: The authors declare that they have no competing interests.

Data Availability

Data will be made available on request.

Supplementary Materials

Texts S1 to S2
Tables S1 to S5
Fig. S1
References [50,51]

References

1. Wen Z, Xu W, Li Q, Han MJ, Tang AH, Zhang Y, Luo XS, Shen JL, Wang W, Li KH, et al. Changes of nitrogen deposition in China from 1980 to 2018. *Environ Int*. 2020;144: Article 106022.
2. Zhang BJ, Li ZX, Feng Q, Gui J, Zhao Y, Zhang BT. Environmental significance of atmospheric nitrogen deposition in the transition zone between the Tibetan plateau and arid region. *Chemosphere*. 2022;307:Article 136096.
3. Wen Z, Ma X, Xu W, Si RT, Liu L, Ma R, Zhao YH, Tang AH, Zhang YY, Wang K, et al. Combined short-term and long-term emission controls improve air quality sustainably in China. *Nat Commun*. 2024;15(1):5169.
4. Du CJ, Guo QJ, Zhang J. A review on moss nitrogen and isotope signatures evidence for atmospheric nitrogen deposition. *Sci Total Environ*. 2022;806:Article 150765.
5. Liu L, Wen Z, Liu S, Zhang XY, Liu XJ. Decline in atmospheric nitrogen deposition in China between 2010 and 2020. *Nat Geosci*. 2024;17(8):733–736.
6. Xue J, Li ZX, Feng Q, Li ZJ, Gui J, Li YC. Ecological conservation pattern based on ecosystem services in the Qilian Mountains, Northwest China. *Environ Dev*. 2023;46:Article 100834.
7. Gao Q, Zhang XY, Liu L, Lu XH, Wang YY. A database of atmospheric inorganic nitrogen deposition fluxes in China from satellite monitoring. *Sci Data*. 2023;10(1):698.
8. Hong SY, Chen J, Biswas A, Cao JJ, Dong XG. Leaf stoichiometry of common species along altitude gradients in the Qilian Mountains, China. *J Plant Ecol*. 2024;17(1): Article rtad044.
9. Zong N, Shi PL, Song MH, Zhang XZ, Jiang J, Chai X. Nitrogen critical loads for an alpine meadow ecosystem on the Tibetan plateau. *Environ Manag*. 2016;57(3):531–542.
10. Harmens H, Schnyder E, Thöni L, Cooper DM, Mills G, Leblond S, Mohr K, Poikolainen J, Santamaria J, Skudnik M, et al. Relationship between site-specific nitrogen concentrations in mosses and measured wet bulk atmospheric nitrogen deposition across Europe. *Environ Pollut*. 2014;194:50–59.
11. Varela Z, Boquete MT, Fernández JA, Martínez-Abaigar J, Núñez-Olivera E, Aboal JR. Mythbusters: Unravelling the pollutant uptake processes in mosses for air quality biomonitoring. *Ecol Indic*. 2023;148:Article 110095.
12. Liu XY, Xiao HY, Liu CQ, Li YY, Xiao HW. Tissue N content and ^{15}N natural abundance in epilithic mosses for indicating atmospheric N deposition in the Guiyang area, SW China. *Appl Geochem*. 2008;23(9):2708–2715.
13. Huang H, Song W, Liu XY. Significant contributions of combustion-related NH_3 and non-fossil fuel NO_x to elevation of nitrogen deposition in southwestern China over past five decades. *Glob Chang Biol*. 2021;27(18):4392–4402.
14. Li JY, Dong YP, Wang Y, Deng TY, Zhao ZT. Moss differentiating the fluxes and sources of nitrogen deposition between 1984 and 2021 in a mountain area of northern China. *Chemosphere*. 2024;362:Article 142684.
15. Harmens H, Norris DA, Cooper DM, Mills G, Steinnes E, Kubin E, Thöni L, Aboal JR, Alber R, Carballeira A, et al. Nitrogen concentrations in mosses indicate the spatial distribution of atmospheric nitrogen deposition in Europe. *Environ Pollut*. 2011;159(10):2852–2860.
16. Harmens H, Norris DA, Sharps K, Mills G, Alber R, Aleksiayenak Y, Blum O, Cucu-Man SM, Dam M, De Temmerman L, et al. Heavy metal and nitrogen concentrations in mosses are declining across Europe whilst some "hotspots" remain in 2010. *Environ Pollut*. 2015;200:93–104.
17. Delgado V, Ederra A, Santamaría JM. Nitrogen and carbon contents and $\delta^{15}N$ and $\delta^{13}C$ signatures in six bryophyte species: Assessment of long-term deposition changes (1980-2010) in Spanish beech forests. *Glob Chang Biol*. 2013;19(7):2221–2228.
18. Wang Y, Dong YP, Ren ZJ, Hu L, Deng TY, Zhao ZT. Mosses record historical variations of atmospheric nitrogen deposition in a mountain area of northern China. *J Plant Ecol*. 2025;18(3):rtaf039.
19. Solga A, Eichert T, Frahm JP. Historical alteration in the nitrogen concentration and ^{15}N natural abundance of mosses in Germany: Indication for regionally varying changes in atmospheric nitrogen deposition within the last 140 years. *Atmos Environ*. 2006;40(40):8044–8055.
20. Dong YP, Liu XY, Sun XC, Song W, Zheng XD, Li R, Liu CQ. Inter-species and intra-annual variations of moss nitrogen utilization: Implications for nitrogen deposition assessment. *Environ Pollut*. 2017;230:506–515.
21. Dong YP, Huang H, Song W, Sun XC, Wang M, Zhang W, Wang KL, Liu CQ, Liu XY. Natural ^{13}C and ^{15}N abundance of moss-substrate systems on limestones and sandstones in a karst area of subtropical China. *Catena*. 2019;180:8–15.
22. Liu XY, Xiao HY, Liu CQ, Li YY. $\delta^{13}C$ and $\delta^{15}N$ of moss *Haplocladium microphyllum* (Hedw.) broth. For indicating growing environment variation and canopy retention on atmospheric nitrogen deposition. *Atmos Environ*. 2007;41(23):4897–4907.
23. Xiao HY, Tang CG, Xiao HW, Liu XY, Liu CQ. Mosses indicating atmospheric nitrogen deposition and sources in the Yangtze River drainage basin, China. *J Geophys Res Atmos*. 2010;115(D14):Article 2009JD012900.
24. Liu XY, Wu D, Song X, Dong YP, Chen CJ, Song W, Liu CQ, Koba K. A non-steady state model based on dual nitrogen and oxygen isotopes to constrain moss nitrate uptake and reduction. *J Geophys Res Biogeosciences*. 2020;125(6): Article e2019JG005498.
25. Liu XY, Koba K, Makabe A, Li XD, Yoh M, Liu CQ. Ammonium first: Natural mosses prefer atmospheric ammonium but vary utilization of dissolved organic nitrogen depending on habitat and nitrogen deposition. *New Phytol*. 2013;199(2):407–419.
26. Li ZX, Feng Q, Li ZJ, Wang XF, Gui J, Zhang BJ, Li YC, Deng XH, Xue J, Gao WD, et al. Reversing conflict between humans and the environment—The experience in the Qilian Mountains. *Renew Sust Energ Rev*. 2021;148:Article 111333.

27. Wu YH, Gao C, Tan BC. The bryophytes of Gansu Province, China: A new annotated checklist. *Arctoa*. 2002;11:11–22.
28. Wang TY, Guan FR, Wang Q, Wu YH. Study on bryophyte species diversity in different landscapes in Qilian Mountain. *Plant Sci J*. 2015;33(4):466–471.
29. Wu Q, L LH, Z KH, Z WJ, L SY. Spatial heterogeneity of bryophyte-litter composition at large-plot scale in *Picea crassifolia* forest in the Qilian Mountains, China. *Mountain Res*. 2025;43(2):185–194.
30. Fu YD, Xu W, Wen Z, Han MJ, Sun JH, Tang AH, Liu XJ. Enhanced atmospheric nitrogen deposition at a rural site in Northwest China from 2011 to 2018. *Atmos Res*. 2020;245:Article 105071.
31. Liu XY, Koba K, Liu CQ, Li XD, Yoh M. Pitfalls and new mechanisms in moss isotope biomonitoring of atmospheric nitrogen deposition. *Environ Sci Technol*. 2012;46(22):12557–12566.
32. Liu XY, Koba K, Yoh M, Liu CQ. Nitrogen and oxygen isotope effects of tissue nitrate associated with nitrate acquisition and utilisation in the moss *Hypnum plumaeforme*. *Funct Plant Biol*. 2012;39(7):598–608.
33. Wang Z, Feng DF, Liu X, Hu B, Bao WK. Biogeographical patterns of community-level content of N and P and their stoichiometric ratios in subtropical forest floor bryophytes. *Ecol Indic*. 2022;143:Article 109369.
34. Liu XY, Xiao HY, Liu CQ, Li YY, Xiao HW. Atmospheric transport of urban-derived NH_x: Evidence from nitrogen concentration and $\delta^{15}N$ in epilithic mosses at Guiyang, SW China. *Environ Pollut*. 2008;156(3):715–722.
35. Li K, Bai KX. Spatiotemporal associations between $PM_{2.5}$ and SO_2 as well as NO_2 in China from 2015 to 2018. *Int J Environ Res Public Health*. 2019;16(13):Article 2352.
36. Shi Y, Xia YF, Lu BH, Liu N, Zhang L, Li SJ, Li W. Emission inventory and trends of NO_x for China, 2000–2020. *J Zhejiang Univ-Sci A*. 2014;15(6):454–464.
37. Zhang X, Zou T, Lassaletta L, Mueller ND, Tubiello FN, Lisk MD, Lu C, Conant RT, Dorich CD, Gerber J, et al. Quantification of global and national nitrogen budgets for crop production. *Nat Food*. 2021;2(7):529–540.
38. Liu XY, Xiao HY, Liu CQ, Li YY, Xiao HW. Stable carbon and nitrogen isotopes of the moss *Haplocladium microphyllum* in an urban and a background area (SW China): The role of environmental conditions and atmospheric nitrogen deposition. *Atmos Environ*. 2008;42(21):5413–5423.
39. Xiao HY, Liu CQ. Estimates of dry and wet deposition using tissue N contents and^{15}N natural abundance in epilithic mosses in atmospheric NH_y-dominated areas. *J Geophys Res Atmos*. 2011;116(D3):Article 2010JD015231.
40. Liu XJ, Duan L, Mo JM, Du EZ, Shen JL, Lu XK, Zhang Y, Zhou XB, He CN, Zhang FS. Nitrogen deposition and its ecological impact in China: An overview. *Environ Pollut*. 2011;159(10):2251–2264.
41. Zhang Q, Zheng YX, Tong D, Shao M, Wang SX, Zhang YH, Xu XD, Wang JN, He H, Liu WQ, et al. Drivers of improved $PM_{2.5}$ air quality in China from 2013 to 2017. *Proc Natl Acad Sci USA*. 2019;116(49):24463–24469.
42. Li C, Ren MX, Cheng H, Chen X, Dong XL, Wei XP, Zheng LG. Uptake patterns for nitrogen and sulfur source by aquatic plants and various nitrogen acquisition strategies: Affected by mining activities. *J Environ Manag*. 2024;354:Article 120436.
43. Zuo YF, Li YH, He KN, Wen YS. Temporal and spatial variation characteristics of vegetation coverage and quantitative analysis of its potential driving forces in the Qilian Mountains, China, 2000–2020. *Ecol Indic*. 2022;143: Article 109429.
44. Liu JX, Fan XW, Li XY, Zheng YP, Li Y, Cui CX, Bai ZH, Ma L, Zhai BN, Li ZY. Responses of different agricultural structures to nitrogen loss and agricultural green development in Northwest China. *Agric Ecosyst Environ*. 2024;367:Article 108956.
45. Liu XY, Yin YM, Song W. Nitrogen isotope differences between major atmospheric NO_y species: Implications for transformation and deposition processes. *Environ Sci Technol Lett*. 2020;7(4):227–233.
46. Zackrisson O, DeLuca TH, Nilsson MC, Sellstedt A, Berglund L. Nitrogen fixation increases with successional age in boreal forests. *Ecology*. 2004;85(12):3327–3334.
47. Dong YP. Mechanisms of carbon and nitrogen concentrations and stable isotope variations in terrestrial mosses [dissertation]. [Tianjin (China)]: Tianjin University; 2019.
48. Yu GR, Jia YL, He NP, Zhu JX, Chen Z, Wang QF, Piao SL, Liu XJ, He HL, Guo XB, et al. Stabilization of atmospheric nitrogen deposition in China over the past decade. *Nat Geosci*. 2019;12(6):424–429.
49. Xie ZY, Xiao HY, Zhu RG, Wu DS. Nitrogen concentrations and stable isotope in epilithic mosses to investigate atmospheric N deposition and n sources in Jiangxi province. *Environ Sci*. 2011;32(04):943–948.
50. Zhu JX, He NP, Wang QF, Yuan GF, Wen D, Yu GR, Jia YL. The composition, spatial patterns, and influencing factors of atmospheric wet nitrogen deposition in Chinese terrestrial ecosystems. *Sci Total Environ*. 2015;511:777–785.
51. Xu W, Luo XS, Pan YP, Zhang L, Tang AH, Shen JL, Zhang Y, Li KH, Wu QH, Yang DW, et al. Quantifying atmospheric nitrogen deposition through a nationwide monitoring network across China. *Atmos Chem Phys*. 2015;15(21):12345–12360.

Ecosystem Health and Sustainability
A SCIENCE PARTNER JOURNAL

#15N Differences between Terricolous and Epilithic Mosses: Implications for Atmospheric Nitrogen Deposition Monitoring

Tong-Yue Deng, Yu-Ping Dong, Yang Wang, Jia-Yi Li, and Lu-Lu Zhang

Citation: Deng T, Dong Y, Wang Y, Li J, Zhang L. #15N Differences between Terricolous and Epilithic Mosses: Implications for Atmospheric Nitrogen Deposition Monitoring. *Ecosyst Health Sustain*. 2025;**11**:0458. DOI: 10.34133/ehs.0458

Terricolous mosses and epilithic mosses are often used to indicate atmospheric nitrogen (N) deposition, while terricolous mosses also absorb N from soils. How to use N isotopes (#15N) of terricolous mosses to trace the levels and sources of atmospheric N deposition accurately is an urgent problem to resolve. Based on the N contents (N_{moss}) and isotopes (#15N_{moss}) of terricolous and epilithic mosses collected in Mount Qilian in 2022, we established a bottom-up method to calculate local atmospheric N deposition levels and source contributions. No significant difference was found in N_{moss} between soils and bare rocks, while terricolous mosses had significantly higher #15N_{moss} than epilithic mosses. Thus, the effects of soil N sources on #15N_{moss} of terricolous mosses should be excluded before they are used to trace emission sources of atmospheric N deposition. The flux of total inorganic N deposition in Mount Qilian was 15.0 ± 2.3 kg N ha#1 year#1, with nitrate-N deposition being dominant. According to analyses of emission sources, it was volatilization-related ammonia (61.9% ± 19.8%; mainly from fertilizer application and wastes) rather than combustion-related ammonia (38.1% ± 19.8%) that dominated atmospheric ammonium-N deposition. It was fossil fuel N oxides (51.5% ± 19.6%; mainly from oil and coal combustion) rather than non-fossil fuel N oxides (48.5% ± 19.6%; mainly from biomass burning and microbial N cycles) that dominated nitrate-N deposition in this region. The Mount Qilian region holds an important position as a crucial ecological barrier in western China. Therefore, it is important to reduce reactive N emissions based on the above source apportionments to protect the fragile ecosystems of Mount Qilian.

View the article online
https://spj.science.org/doi/10.34133/ehs.0458

Ecosystem Health and Sustainability (ISSN 2332-8878) is published by the American Association for the Advancement of Science. 1200 New York Avenue NW, Washington, DC 20005.